Light damage induces inflammatory factors in mouse retina and vitreous humor

Wei Liu, Xingfei Zhu, Xiangyu Ge, Yulin Chen, David Wan-Cheng Li, Lili Gong

(Wei Liu and Xingfei Zhu contributed equally to this work.)

State Key Laboratory of Ophthalmology, Zhongshan Ophthalmic Center, Sun Yat-Sen University, Guangzhou, Guangdong, 510060, China

Purpose: Increased inflammatory factor levels have been reported in the vitreous humor (VH) of diabetic retinopathy and neovascular age-related macular degeneration, ocular diseases generally associated with the formation of new retinal blood vessels and leakage. However, the levels of inflammatory mediators are less known in retinal degeneration without neovascularization. Human retinitis pigmentosa (RP) and animal models of light-induced retinal degeneration (LIRD) share several features, such as photoreceptor death and retinal inflammation. Here, we aimed to determine the levels of inflammatory factors in the VH of the LIRD mouse model.
Methods: LIRD was induced by exposing BALB/c mice to white light (15,000 lx, 2 h), and the mice were recovered for 2 days before analysis (n = 50 mice). We assessed retinal morphology using optical coherence tomography and hematoxylin and eosin staining; retinal cell viability was determined using terminal deoxynucleotidyl transferase dUTP nick-end labeling, and retinal responses were measured based on electroretinogram signals. Total retinal RNAs were extracted and subjected to RNA sequencing analysis. VH samples from control (n = 4) and LIRD mice (n = 9) were assayed in triplicate for a panel of four inflammatory mediators using the Simple Plex Cartridge on an Ella System.
Results: Retinal degeneration, photoreceptor death, infiltration of microglia/macrophages into the photoreceptor layer, and loss of a- and b-waves were obviously detected after LIRD. RNA sequencing revealed that light damage (LD) led to the significant upregulation of inflammatory factors in mouse retinas. In the VH, LD increased the total protein concentration. Dramatic induction of CCL2 (~3000 fold) and IL6 (~10 fold) was detected in VH in response to LD. Increased but not significant levels of TNFα and IL1β were also detected in light-exposed VH.
Conclusions: Given that the LIRD model mimics RP pathogenesis in some aspects, these results suggest a causative link between retinal degeneration and VH inflammation in RP progression, and the increased CCL2 level in VH may reflect similar elevated CCL2 expression in the degenerative retina.

The vitreous humor (VH) is a clear and transparent liquid/gel mixture in the posterior cavity of the eye. It directly contacts the retina; therefore, the components of VH reflect the physiologic or pathogenic conditions of the retina in some respects. Previous studies have shown that VH RNA or protein profiles are associated with different spectrums of retinal diseases. For example, several microRNAs are enriched in VH and are correlated with specific ocular pathologies [1]. Proteins involved in angiogenesis, immune response, and oxygen-induced vessel loss have been detected in the VH of proliferative diabetic retinopathy patients [2,3]. The extracellular chaperone clusterin, pigment epithelium-derived factor opticin, and transport proteins for lipophilic substances prostaglandin-H2 D-isomerase in VH have been proposed as biomarkers for neovascular age-related macular degeneration [4].

Retinitis pigmentosa (RP) is a highly heterogeneous retinal dystrophy characterized by primary degeneration of photoreceptors, followed by death of inner retinal neurons [5,6]. Photoreceptor loss accompanied by chronic retinal inflammation has been detected in various human patients and RP animal models [7-9], and the inflammatory status can persist even after photoreceptor loss [10]. Inflammatory cells in the anterior vitreous cavity were observed in patients with RP, and elevated pro-inflammatory cytokines, such as IL1β and IL6, were detected in the VH of patients with RP [9,11]. The sustained inflammatory environment is proposed to exacerbate photoreceptor loss and retinal degeneration in RP, as aberrant active immune cells, that is, reactive retinal microglia, are found in phagocyte live photoreceptors [12,13].

Although VH has been well studied in animal models of diabetic retinopathy and neovascular age-related macular

Correspondence to: Lili Gong, State Key Laboratory of Ophthalmology, Zhongshan Ophthalmic Center, Sun Yat-Sen University, Guangzhou, Guangdong, 510230, China. gonglili@gzzoc.com

degeneration (nAMD), in which neovascularization usually occurs, the components of VH are less known in RP mouse models. Identifying the inflammatory mediators in VH under RP pathogenic conditions is important because they could highlight a causal link between retinal inflammation and inflammatory factors secreted into VH, as well as provide potential biomarkers that represent changes in proteins during retinal degeneration. Here, we used a light-induced retinal degeneration (LIRD) mouse model to mimic RP and found global upregulated protein concentrations in VH after light damage (LD). Concomitant with LD-induced inflammatory factor expression in the retina, significantly increased chemokine (C-C motif) ligand 2 (CCL2) levels were detected in the VH after LD.

METHODS

Experimental animals, reagents, and antibodies: BALB/c mice (5–8 weeks) purchased from Sun Yat-Sen University Laboratory Animal Center were used for all experiments. Mice were housed under a 12:12 light:dark cycle with ad libitum access to standard mouse chow. The study included 50 mice, with an equal distribution of males and females. All procedures conformed according to the ARVO Statement for the Use of Animals in Ophthalmic and Vision Research and were approved by the Animal Use and Care Committee of Zhongshan Ophthalmic Center at the Sun Yat-Sen University, Guangzhou, China (Approval form #2022031). The reagents, antibodies, and other resources used in this study are listed.

Light exposure: The mice were placed in constant darkness 12 h before exposure to light. Non-anesthetized mice were then exposed to typical laboratory lighting (50 lx) or white light (15,000 lx) for 2 h using light-emitting diode (LED) lights placed at the top of a standard mouse cage. To maintain orientation during light exposure, each mouse was placed inside an end-cut 50 ml conical tube, which was secured inside a box used for light exposure. During light exposure, the mouse's front and hind paws were fixed with tape to ensure that the mouse's body did not flip over. The level of illumination was measured using a digital light meter (TASI, T8121, Jiangsu, China).

RNA-seq analysis: Mice were exposed with or without bright light (15,000 lx, 2 h), and retinas were collected 48 h after exposure. Total RNAs were extracted using TRIzol. The purified RNAs were then sent to Chi Biotech for sequencing. Bulk RNA-seq data were accessed from the NCBI Sequence Read Archive (SRA) database under accession number PRJNA916821. Adapters were removed using Trim Galore v1.18. Raw sequencing data were mapped to the GRCm39 genome assembly using HISAT2 v2.2.1 [14]. We calculated fragments per kilobase of exon per million (FPKM) using featureCounts v2.0.1 [15]. Using DESeq2 [16], we identified differentially expressed genes (DEGs) between control and light damage groups (fold change ≥2 and false discovery rate [FDR] ≤0.05). All upregulated genes (fold change ≥2 and FDR ≤0.05; n = 1384) were used for gene set enrichment analysis (GSEA) by R package clusterProfiler [17].

Immunofluorescence (IF) staining and in situ terminal deoxy-nucleotidyl transferase dUTP nick-end labeling (TUNEL) assay: After euthanasia, the eyeballs were enucleated into PBS to remove excess connective tissue and fixed in 4% PFA for 10 min. A small cut was made in the cornea of each mouse eye after fixation for 10 min and further fixation for 50 min. The eye was then dehydrated using 10% and 20% sucrose in 0.1 M phosphate-buffered saline for 1 h and dehydrated in 30% sucrose overnight. The dehydrated eyes were placed in a 1:1 mixture of 30% sucrose and optimal cutting temperature for 1 h before being embedded in the optimal cutting temperature medium. Retinal cryosections along the superior and inferior retinal meridians were cut at 8-μm thickness, and the sections were subjected to standard immunofluorescence protocols, as previously described [18]. The antibodies and dilution conditions are as follows: rabbit monoclonal (EPR16588) to IBA1 (Abcam, # ab178846), 1:100; Anti-rabbit IgG (H+L), F (ab') 2 Fragment (Alexa Fluor ® 594 Conjugate; Cell Signaling Technology, #8889), 1:500. TUNEL assay was performed using a TUNEL BrightRed Apoptosis Detection Kit (Vazyme, #A113) according to the manufacturer's procedure. The stained retinal sections were imaged with TissueFAXS microscopy.

Coomassie blue assay: The VH was diluted with radioim-munoprecipitation (RIPA) assay buffer (VH: RIPA = 1:1) containing a proteinase inhibitor cocktail and a protein phosphatase inhibitor. An equal volume of VH was used for electrophoresis. After electrophoresis, the gel was fixed/stained with 0.05% Coomassie brilliant blue R-250 prepared in 50% methanol and 10% acetic acid. Staining was performed for 4 h at room temperature with gentle shaking. The gel was then washed in a washing buffer (50% methanol, 10% acetic acid) for 24 h, and images were taken using a Bio-Rad imaging system.

Optical coherence tomography (OCT): Before imaging, the mice were anesthetized with 1% pentobarbital sodium (70 μl/10 g, prepared in normal saline solution). Their pupils were dilated with 1–2 drops of tropicamide phenylephrine eye drops, and the corneas were lubricated with normal saline solution. OCT was performed on both eyes with a Heidelberg Spectralis OCT device (Heidelberg Engineering) to investigate structural changes. Thickness measurements were
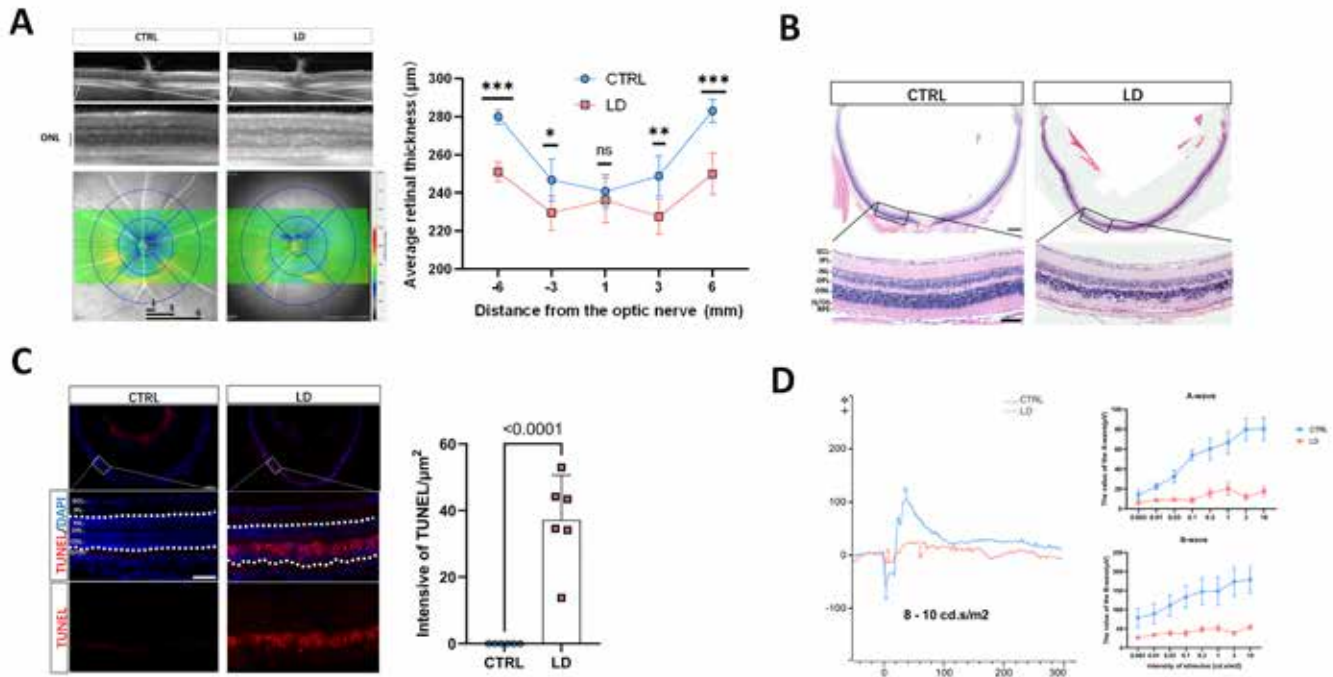
Figure 1. LD leads to retinal degeneration and photoreceptor death. The mice were exposed to typical laboratory lighting (50 lx) or white light (15,000 lx) for 2 h, and analyses were performed two days after LD. **A**: In vivo OCT shows retina structure in control (CTRL) and light-exposed (LD) mice. LD induces an altered reflectance in the outer nuclear layer (ONL); n = 5 mice per group. **B**: HE staining shows retina structure in CTRL and LD mice. Scale bar: upper panel: 200 μm, lower panel: 50 μm. GCL: ganglion cell layer; IPL: inner plexiform layer; INL: inner nuclear layer; OPL: outer plexiform layer; ONL: outer nuclear layer; IS: inner segment; OS: outer segment; n = 3 mice per group. **C**: TUNEL assay shows cell viability in CTRL and LD mouse retinas. Note that LD causes massive cell death in photoreceptors (red signals), but no detectable cell death occurs in other retinal layers. Scale bar: upper panel: 200 μm, lower panel: 50 μm. The right panel shows the quantification results of TUNEL. The TUNEL signal was quantified by dividing the fluorescence intensity by the area of INL+OPL+ONL (region indicated by dashed lines) using ImageJ. Six regions from four retinas were randomly selected for quantification. Unpaired *t*-test, n = 4 eyes per group. **D**: ERG response of mouse retina with the indicated treatment; n = 4–6 mice per group.

performed with a circular ring scan (circle diameter 1, 3, and 6 ETDRS) centered on the optic nerve head, which represents the average retinal thickness in a certain field. Central retinal thickness was calculated from four fields around the optic nerve head using Heidelberg Eye Explorer software.

Electroretinography (ERG): Briefly, the mice were dark-adapted overnight and anesthetized with 1% pentobarbital sodium. Their pupils were dilated with 1–2 drops of tropicamide phenylephrine eye drops, and the corneas were lubricated with hypromellose gel. The ERG was recorded using a Diagnosys Celeris rodent ERG device. Electrodes were placed on top of each cornea. Mice were stimulated with flashlight of various intensities, ranging from 0.003 to 10 cd sec/m^2.

Hematoxylin and eosin (HE) staining of the retina: After euthanasia, the eyeballs were enucleated and fixed in FAS eye fixation solution (Servicebio #G1109) for 24 h. After fixation, the eyes were dehydrated in 60%, 70%, 80%, 90%, and 100% ethanol and processed for paraffin embedding. Paraffin sections of 8-μm thickness were subjected to hematoxylin and eosin (HE) staining, as previously described [18]. The stained retinal sections were imaged with TissueFAXS microscopy.

ELLA analysis: The VH was obtained using a Hamilton needle, with a volume of 3–5 μl obtained from each eye. VH from the control (n = 4 mice) and LIRD mice (n = 9 mice) were diluted 2–10 times and loaded in a total of 50 μl volume, assayed in triplicate for a panel of four inflammatory mediators using the Simple Plex Cartridge (ProteinSimple, SPCKC-MP-004230) on an Ella™ System (ProteinSimple). Data were acquired on Simple Plex Explorer with an instrument default setting.

Statistics: The results are expressed as the mean ± SD. GraphPad Prism 9 software (GraphPad software, Inc., La Jolla, CA) was used for statistical analysis, as described in the Results section. All tests are two-tailed, unpaired *t*-tests unless otherwise indicated.

Ethics approval and consent to participate: All procedures conformed according to the ARVO Statement for the Use of Animals in Ophthalmic and Vision Research and were approved by the Animal Use and Care Committee of Zhong-shan Ophthalmic Center with the IACUC at the Sun Yat-Sen University, Guangzhou (#2022031), China.

RESULTS

Light damage induces photoreceptor death, retinal degeneration, and function impairment: We determined the LIRD mouse model using retinal morphological and functional analyses. The BALB/c mice were exposed to bright light, and the effects of LD were first investigated by in vivo OCT imaging. Thinning of the outer nuclear layer (ONL) was evident in the mouse retina after LD (Figure 1A). Histological analysis by HE staining confirmed that LD led to disruption of the retinal structure and loss of photoreceptors (Figure 1B). Further, TUNEL assays demonstrated prominent photoreceptor death after LD (Figure 1C). Concomitant with retinal degeneration and photoreceptor death, ERG analysis showed that the a- and b-wave amplitudes were significantly decreased, indicating LD-induced retinal response impairment (Figure 1D). Together, these results demonstrate the successful establishment of the LIRD mouse model.

LD induces inflammatory responses in the retina: We explored retinal transcriptome alteration in response to LD by RNA sequencing analysis (RNA-seq, n = 4 mice per group). Robust upregulation of inflammatory genes was detected in the mouse retina after LD (Figure 2A). The chemokines *Ccl2*, *Ccl4*, and *Ccl3* ranked top in the profile of upregulated genes (Figure 2A). Our recent study revealed that interferon signaling was increased in sodium iodate-induced retinal degeneration [18]. Interestingly, the interferon-inducible gene *Ifi204*, and *Casp1*, an effector of interferon signaling, were
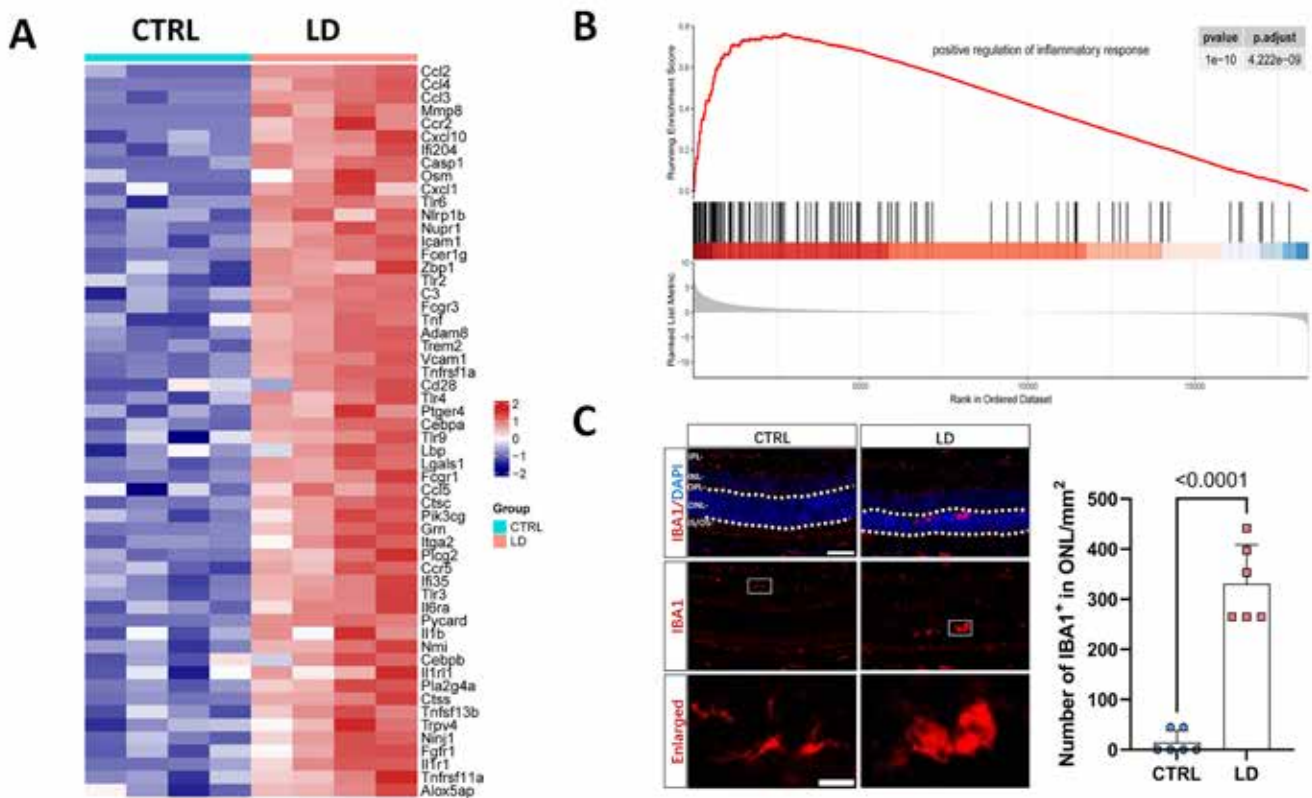

Figure 2. Light damage (LD) induces retinal inflammation and infiltration of microglia/macrophages into the outer nuclear layer (ONL). **A**: A heatmap shows genes for positive regulation of inflammatory response in control (CTRL) and LD mouse retinas. n = 4 mice per group. **B**: Gene set enrichment analysis (GSEA) analysis of the positive regulation of the inflammatory response in response to LD (p. adjust = 4.222e-09). **C**: Immunofluorescence analysis shows IBA1-positive microglia/macrophages. Note that LD induces the migration of IBA1-positive cells to the ONL layer. Right panel: quantification of IBA1-positive cells in ONL. The IBA1-positive cell number was divided by the ONL area (region indicated by dashed lines) using ImageJ. Six regions from four retinas were randomly selected for quantification. Scale bar: upper panel: 50 μm; lower panel: 10 μm. Unpaired *t*-test, n = 4 eyes per group.
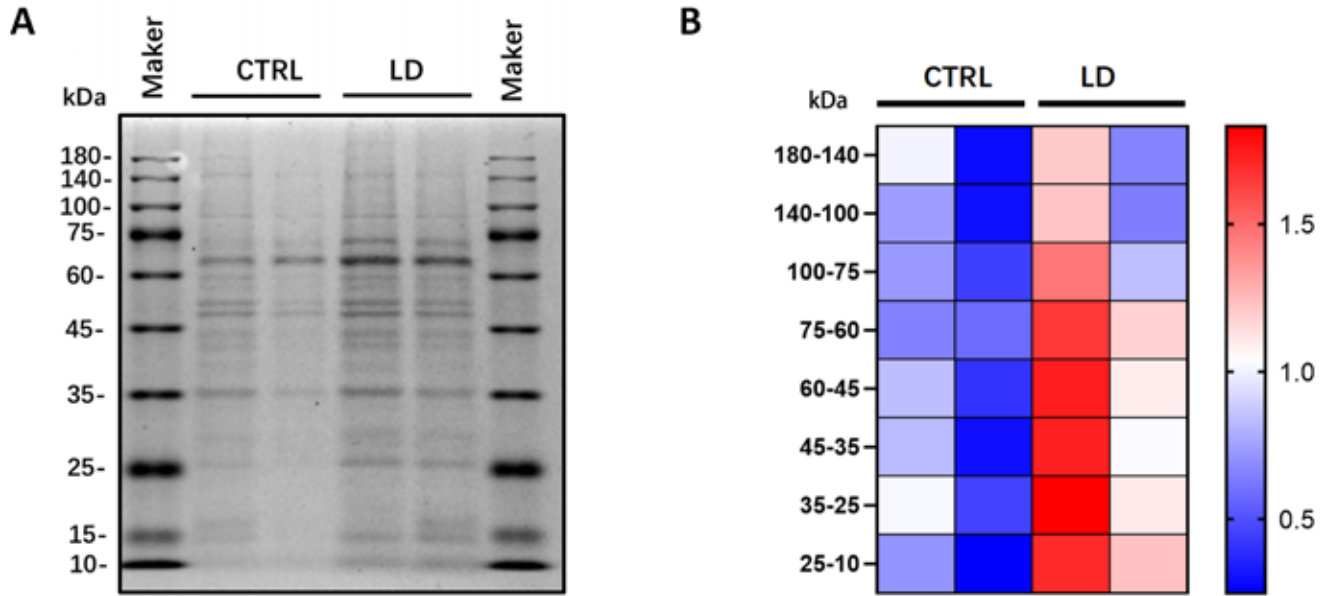
Figure 3. Coomassie blue staining of VH from CTRL and LD mice. (A) The VH samples were collected from CTRL and LD mouse eyes. For each line, an equal volume of VH (2.5 µl) was loaded. (B) The heatmap shows the protein band intensity within the indicated molecular weight ranges. n = 2 eyes per sample. The band intensity was measured using ImageJ.

induced by LD (Figure 2A), suggesting that activation of the interferon pathway may be a shared mechanism in retinal degeneration. Further, metalloproteases (*Mmp8*, *Adam8*), interleukins (*Il1b*), complement components (*C3*), and toll-like receptors (*Tlr6*, *Tlr2*) were also significantly increased by light exposure (Figure 2A). GSEA further demonstrated a significant enrichment of genes in the positive regulation of the inflammatory response (Figure 2B).

Because activation of macrophage/microglia is a hallmark of retinal inflammation, we performed immunohistochemistry staining and labeled the macrophages/microglia with an anti-IBA1 antibody. In the control retina, macrophages/microglia were mainly detected in the inner and outer plexiform, with typical thin and branched processes representing the resting phenotype (Figure 2C). After LD, a substantial increase in IBA1-positive cells was found in the ONL, exhibiting a swollen, amoeboid-like reactive phenotype (Figure 2C). These findings suggest that LD induces an inflammatory response and infiltration of macrophages/microglia in mouse retinas.

Light damage increases VH protein concentration: We then determined the overall VH proteins using Coomassie blue staining. The VH samples were loaded at the same volume, revealing an overall increased protein concentration based on the degree of Coomassie blue staining (Figure 3A), as evidenced by increased band intensity.

Light damage increases inflammatory factor expression in VH: We then measured the VH inflammatory factor using Ella, a highly sensitive automated immunoassay system. We chose a cartridge coated with four inflammatory mediators that were previously reported to be involved in retinitis pigmentosa [9]. In the control group, the mean concentrations of CCL2, IL6, IL1β and TNFα in VH were 118.4 ± 104.8, 1.7 ± 1.2, 9.6 ± 6.8, and 3.1 ± 2.1 pg/ml, respectively (Figure 4A-D). After LIRD, the concentrations of CLL2 (3000.9 ± 1077.0 pg/ml; Figure 4A) and IL6 (9.5 ± 4.1 pg/ml) were increased ~3000- and 10-fold, respectively (Figure 4B). Notably, this dramatic upregulation of CCL2 in the VH of LRID mice is consistent with the results of the RNA-seq analysis that showed CLL2 ranking top among upregulated inflammatory factors in the LD retina (Figure 2A). Increased levels of TNFα (12.6 ± 11.0 pg/ml; Figure 4C) and IL1β (42.3 ± 60.5 pg/ml; Figure 4D) were also detected in the VH after LIRD, although not significant.

DISCUSSION

Our results revealed dramatic upregulation of the inflammatory chemokine CLL2 and cytokine IL6 in VH in response to LD. The source of such inflammatory factors may be derived from the adjacent retina or from infiltrated immune cells, which were reported in the VH of patients with RP [9,11].
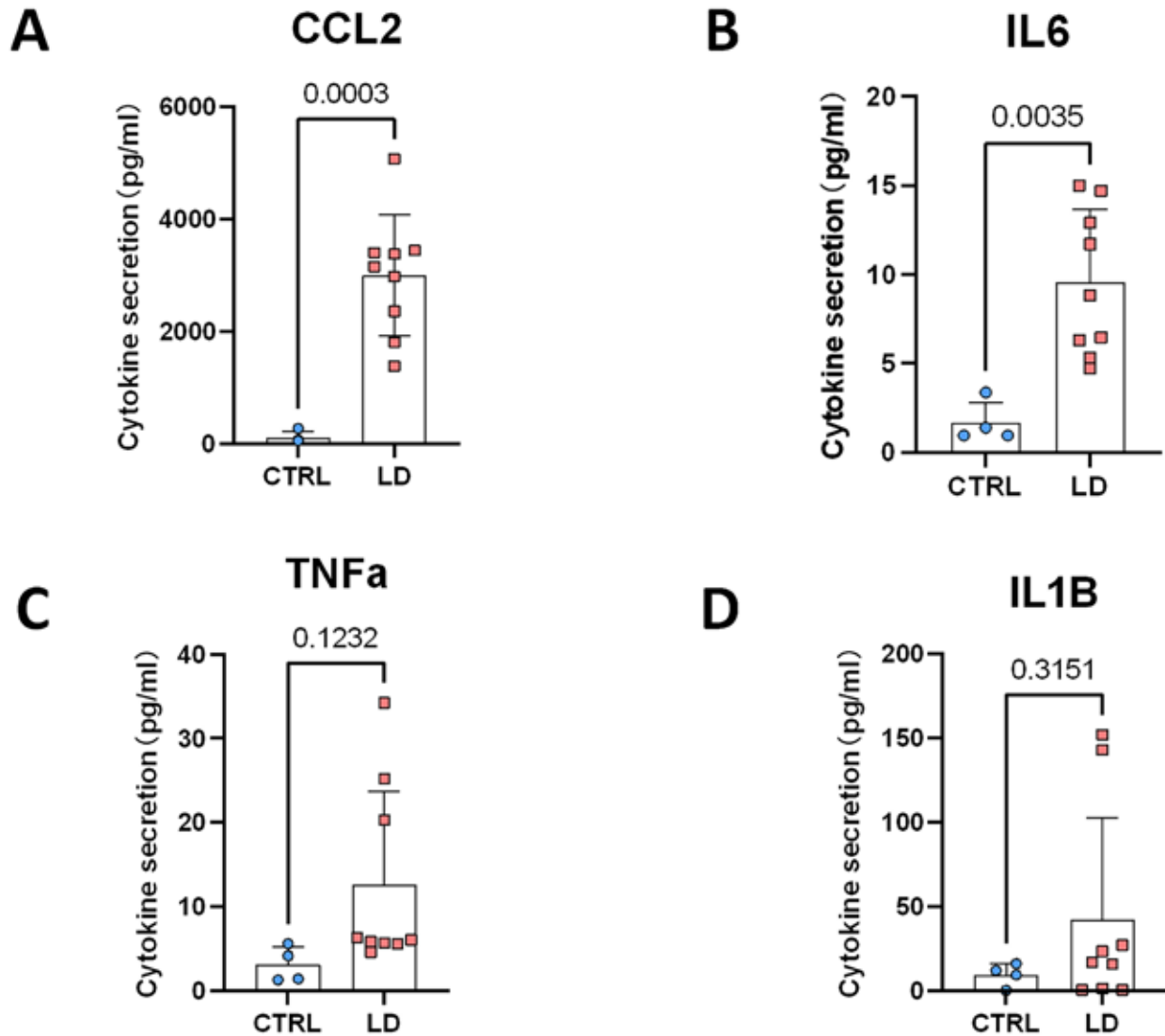
Figure 4. Quantification of inflammatory factors in VH by the Ella system. The VH samples from the CTRL and LD mouse eyes were collected. For the CTRL group, n = 4 mice; for the LD group, n = 9 mice. The *p* value was calculated by an unpaired *t*-test.

CCL2 is a chemokine ligand that acts as a molecular cue for leukocyte homing during retinal inflammation and is increased in retinal degenerations, including AMD and RP [19]. Our results demonstrating a robust upregulation of CCL2 in LD mouse VH are in concert with these clinical observations. However, the type of retinal cells secreting CCL2 into VH is currently unknown. One possibility is the Müller cells, because increased CCL2 mRNA was detected in the Müller cells after light damage [20,21]. Pharmacological suppression of chemokine signaling has been shown to ameliorate subretinal macrophage accumulation and photoreceptor death during retinal degeneration [22]. Our results suggest that the

concentration of CCL2 in VH may reflect the concentration in the retina; therefore, CCL2 levels may be useful for predicting the therapeutic effects of anti-inflammatory drugs in treating RP.

Enhanced IL6 has been detected in many ocular diseases [23,24], and as a proinflammatory cytokine, IL6 is thought to manifest an inflammatory response in retinal diseases [23]. However, the role of IL6 in retinal pathogenesis remains controversial. For example, elevated IL6 in optic nerve head injury enhances nerve damage [25], and IL6 derived from human microglia can inhibit neurosphere generation in vitro [26]. By contrast, IL6 also stimulates retinal ganglion cell

regeneration after optic nerve injury and promotes neuritogenesis in cultured retinal ganglion cells [25,27]. Furthermore, IL6 reportedly protected photoreceptors in an experimental model of retinal detachment [28]. We speculate that the concentration of IL6 may account for its diverse functions in eye pathogenesis. IL6 levels in the VH of patients with RP have been found to be 257.8 ± 488.0 pg/ml [9]. In our study, we found that the VH IL6 level was 9.5 ± 4.1 pg/ml after LD, which was much lower than that in patients with RP. Currently, we do not know whether LD-induced IL6 in VH is neuroprotective or neurodestructive. Future studies using the IL6 neutralization antibody or IL6 knockout mice may help elucidate its function in LIRD.

REFERENCES

1. Ragusa M, Caltabiano R, Russo A, Puzzo L, Avitabile T, Longo A, Toro MD, Di Pietro C, Purrello M, Reibaldi M. MicroRNAs in vitreus humor from patients with ocular diseases. Mol Vis 2013; 19:430-40. [PMID: 23441115].

2. Kim T, Kim SJ, Kim K, Kang UB, Lee C, Park KS, Yu HG, Kim Y. Profiling of vitreous proteomes from proliferative diabetic retinopathy and nondiabetic patients. Proteomics 2007; 7:4203-15. [PMID: 17955474].

3. Wang H, Feng L, Hu JW, Xie CL, Wang F. Characterisation of the vitreous proteome in proliferative diabetic retinopathy. Proteome Sci 2012; 10:15-[PMID: 22390717].

4. Nobl M, Reich M, Dacheva I, Siwy J, Mullen W, Schanstra JP, Choi CY, Kopitz J, Kretz FTA, Auffarth GU, Koch F, Koss MJ. Proteomics of vitreous in neovascular age-related macular degeneration. Exp Eye Res 2016; 146:107-17. .

5. Hartong DT, Berson EL, Dryja TP. Retinitis pigmentosa. Lancet 2006; 368:1795-809. [PMID: 17113430].

6. Newton F, Megaw R. Mechanisms of Photoreceptor Death in Retinitis Pigmentosa. Genes (Basel) 2020; 11:1120-[PMID: 32987769].

7. Zhao L, Hou C, Yan N. Neuroinflammation in retinitis pigmentosa: Therapies targeting the innate immune system. Front Immunol 2022; 13:1059947[PMID: 36389729].

8. Yoshida N, Ikeda Y, Notomi S, Ishikawa K, Murakami Y, Hisatomi T, Enaida H, Ishibashi T. Laboratory evidence of sustained chronic inflammatory reaction in retinitis pigmentosa. Ophthalmology 2013; 120:e5-12. [PMID: 22986110].

9. Yoshida N, Ikeda Y, Notomi S, Ishikawa K, Murakami Y, Hisatomi T, Enaida H, Ishibashi T. Clinical evidence of sustained chronic inflammatory reaction in retinitis pigmentosa. Ophthalmology 2013; 120:100-5. [PMID: 22986109].

10. Noailles A, Maneu V, Campello L, Gomez-Vicente V, Lax P, Cuenca N. Persistent inflammatory state after photoreceptor loss in an animal model of retinal degeneration. Sci Rep 2016; 6:33356-[PMID: 27624537].

11. Albert DM, Pruett RC, Craft JL. Transmission electron microscopic observations of vitreous abnormalities in retinitis pigmentosa. Am J Ophthalmol 1986; 101:665-72. [PMID: 3717249].

12. Zhao L, Zabel MK, Wang X, Ma W, Shah P, Fariss RN, Qian H, Parkhurst CN, Gan WB, Wong WT. Microglial phagocytosis of living photoreceptors contributes to inherited retinal degeneration. EMBO Mol Med 2015; 7:1179-97. [PMID: 26139610].

13. Hume DA, Perry VH, Gordon S. Immunohistochemical localization of a macrophage-specific antigen in developing mouse retina: phagocytosis of dying neurons and differentiation of microglial cells to form a regular array in the plexiform layers. J Cell Biol 1983; 97:253-7. [PMID: 6345555].

14. Kim D, Langmead B, Salzberg SL. HISAT: a fast spliced aligner with low memory requirements. Nat Methods 2015; 12:357-60. [PMID: 25751142].

15. Liao Y, Smyth GK, Shi W. featureCounts: an efficient general purpose program for assigning sequence reads to genomic features. Bioinformatics 2014; 30:923-30. [PMID: 24227677].

16. Love MI, Huber W, Anders S. Moderated estimation of fold change and dispersion for RNA-seq data with DESeq2. Genome Biol 2014; 15:550-[PMID: 25516281].

17. Yu G, Wang LG, Han Y, He QY. clusterProfiler: an R package for comparing biological themes among gene clusters. OMICS 2012; 16:284-7. [PMID: 22455463].

18. Zou M, Ke Q, Nie Q, Qi R, Zhu X, Liu W, Hu X, Sun Q, Fu JL, Tang X, Liu Y, Li DW, Gong L. Inhibition of cGAS-STING by JQ1 alleviates oxidative stress-induced retina inflammation and degeneration. Cell Death Differ 2022; 29:1816-33. .

19. Nagineni CN, Kommineni VK, Ganjbaksh N, Nagineni KK, Hooks JJ, Detrick B. Inflammatory Cytokines Induce Expression of Chemokines by Human Retinal Cells: Role in Chemokine Receptor Mediated Age-related Macular Degeneration. Aging Dis 2015; 6:444-55. [PMID: 26618046].

20. Natoli R, Fernando N, Madigan M, Chu-Tan JA, Valter K, Provis J, Rutar M. Microglia-derived IL-1beta promotes chemokine expression by Muller cells and RPE in focal retinal degeneration. Mol Neurodegener 2017; 12:31-[PMID: 28438165].

21. Rutar M, Natoli R, Valter K, Provis JM. Early focal expression of the chemokine Ccl2 by Muller cells during exposure to damage-inducing bright continuous light. Invest Ophthalmol Vis Sci 2011; 52:2379-88. [PMID: 21228381].

22. Fernando N, Natoli R, Valter K, Provis J, Rutar M. The broad-spectrum chemokine inhibitor NR58–3.14.3 modulates macrophage-mediated inflammation in the diseased retina. J Neuroinflammation 2016; 13:47-[PMID: 26911327].

23. Zahir-Jouzdani F, Atyabi F, Mojtabavi N. Interleukin-6 participation in pathology of ocular diseases. Pathophysiology 2017; 24:123-31. [PMID: 28629694].

24. Krogh Nielsen M, Subhi Y, Molbech CR, Falk MK, Nissen MH, Sorensen TL. Systemic Levels of Interleukin-6 Correlate With Progression Rate of Geographic Atrophy Secondary to Age-Related Macular Degeneration. Invest Ophthalmol Vis Sci 2019; 60:202-8. [PMID: 30644965].

25. Chidlow G, Wood JP, Ebneter A, Casson RJ. Interleukin-6 is an efficacious marker of axonal transport disruption during experimental glaucoma and stimulates neuritogenesis in cultured retinal ganglion cells. Neurobiol Dis 2012; 48:568-81. [PMID: 22884876].

26. Balasubramaniam B, Carter DA, Mayer EJ, Dick AD. Microglia derived IL-6 suppresses neurosphere generation from adult human retinal cell suspensions. Exp Eye Res 2009; 89:757-66. [PMID: 19596318].

27. Fischer D. Hyper-IL-6: a potent and efficacious stimulator of RGC regeneration. Eye (Lond) 2017; 31:173-8. [PMID: 27886185].

28. Chong DY, Boehlke CS, Zheng QD, Zhang L, Han Y, Zacks DN. Interleukin-6 as a photoreceptor neuroprotectant in an experimental model of retinal detachment. Invest Ophthalmol Vis Sci 2008; 49:3193-200. [PMID: 18378582].